Rock-physics templates for clay-rich source rocks

by

José M. Carcione
OGS, Italy
and
Per Avseth
NTNU and Tullow Oil, Norway.

HC generation from source rocks

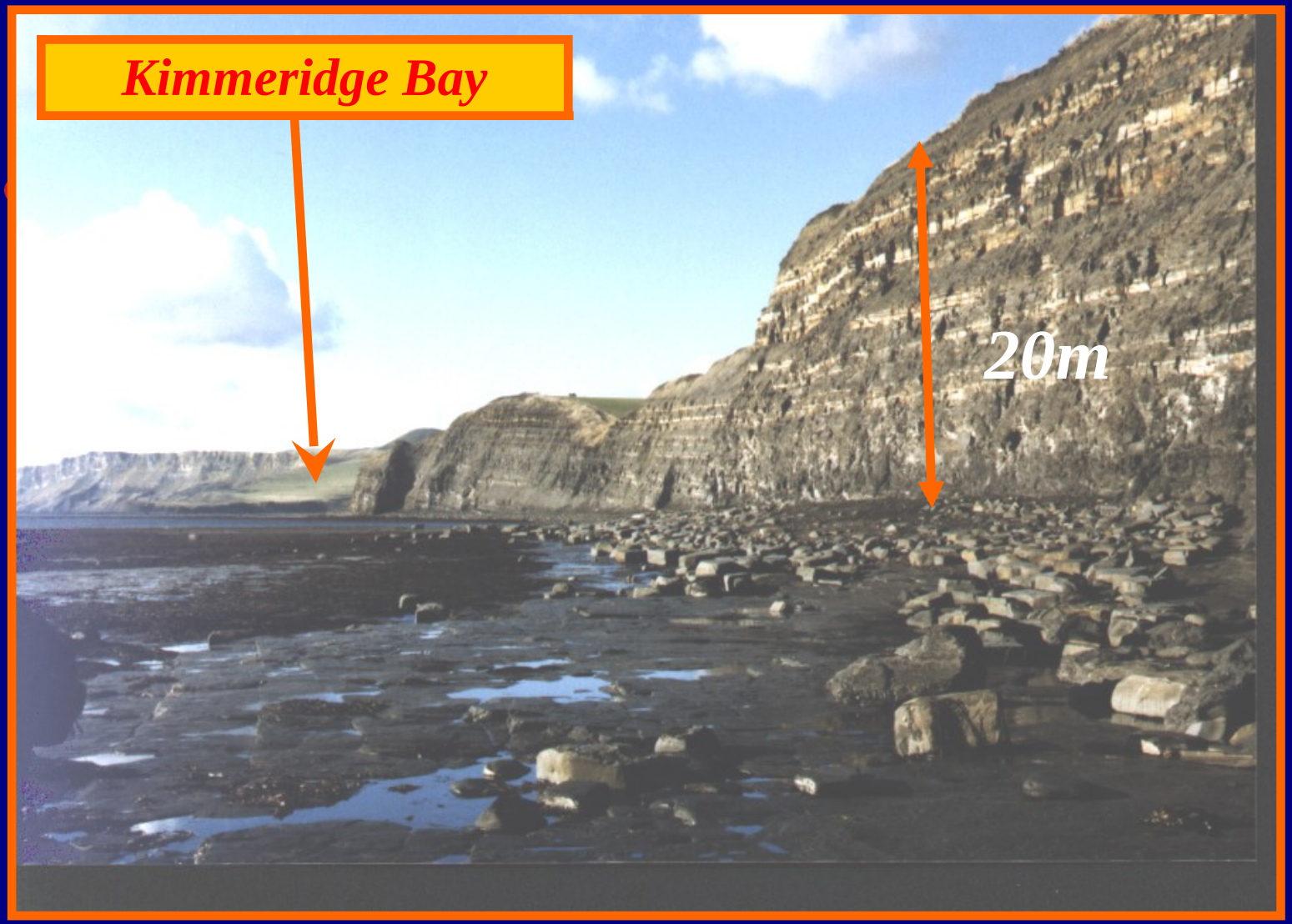

The seismic event

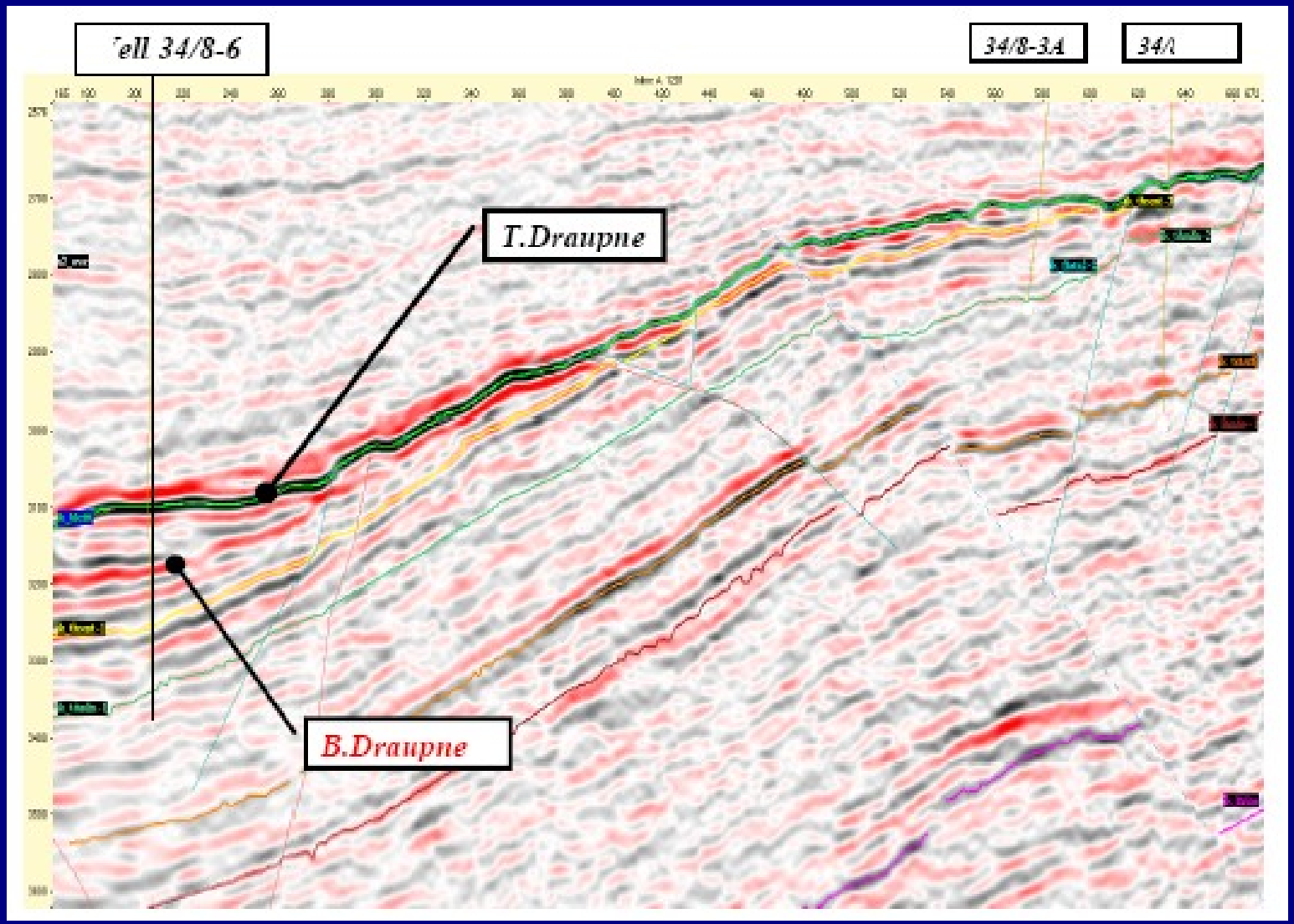

Log profiles

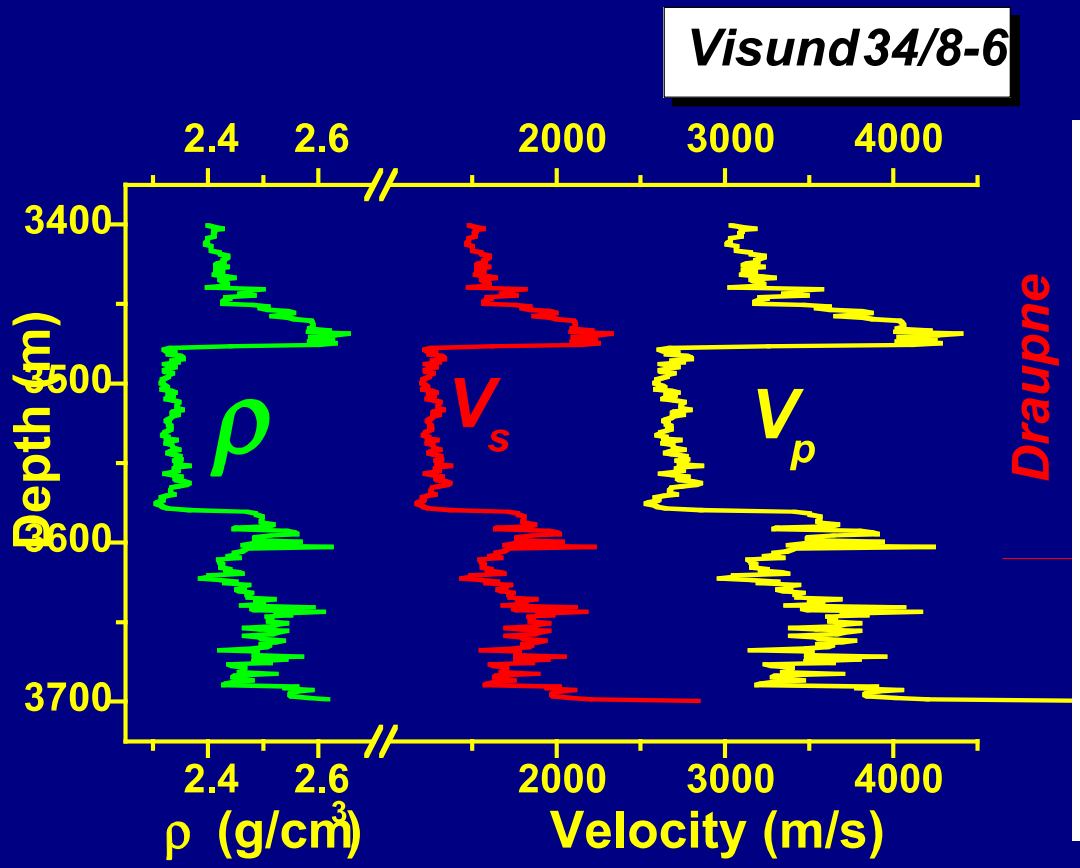

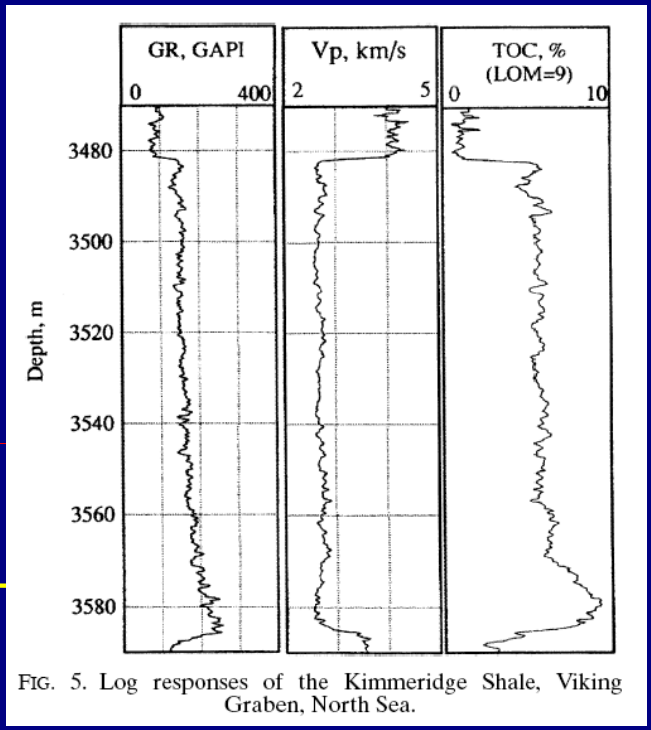

FIG. 5. Log responses of the Kimmeridge Shale, Viking Graben, North Sea.

Kerogen fraction - Kimmeridge shale

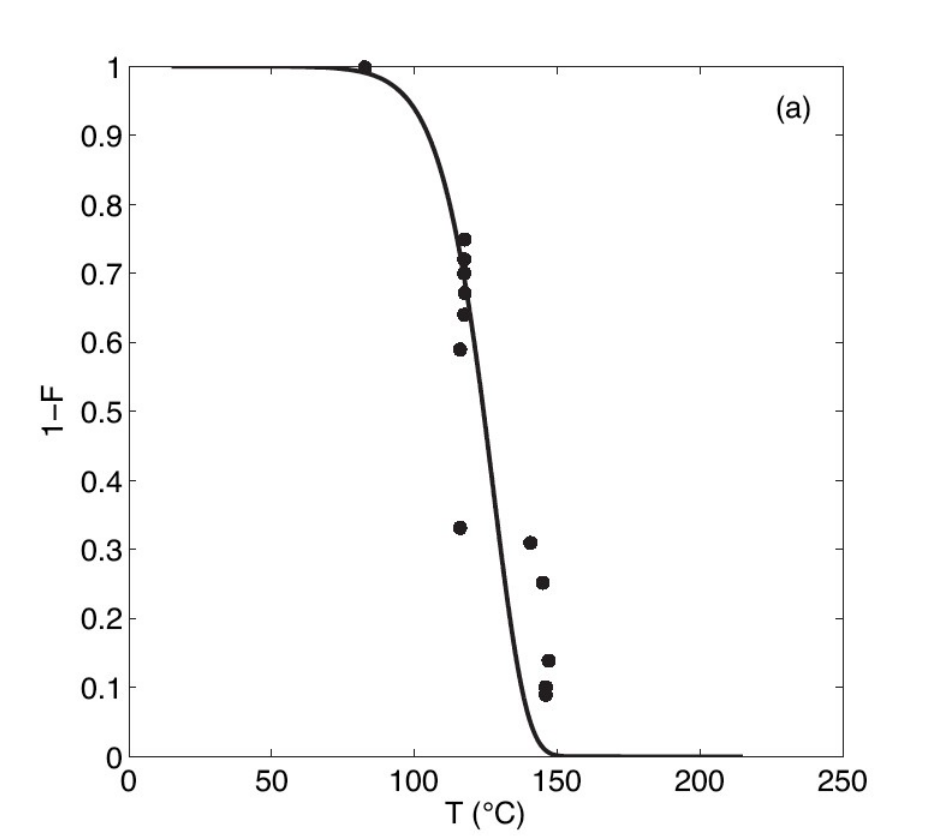

E = 27800 cal/mol
A=10^{14}/m.y.
G=25 ^{o}C/km
S=0.04 mm/y
H=GS=1 ^{o}C/m.y.
Arrhenius 1st -order

Data: Pepper and Corvi (1995)

Carcione, J. M., Helle, H. B., and Avseth, P., 2011, Source-rock seismic-velocity models: Gassmann versus Backus, Geophysics, 76, N37-N45.

Pinna, G., Carcione, J. M., and Poletto, F., 2011 Kerogen to oil conversion in source rocks. Pore-pressure build-up and eects on seismic velocities, Journal of Applied Geophysics, 74, 229-235.

Kerogen/oil fraction *F*

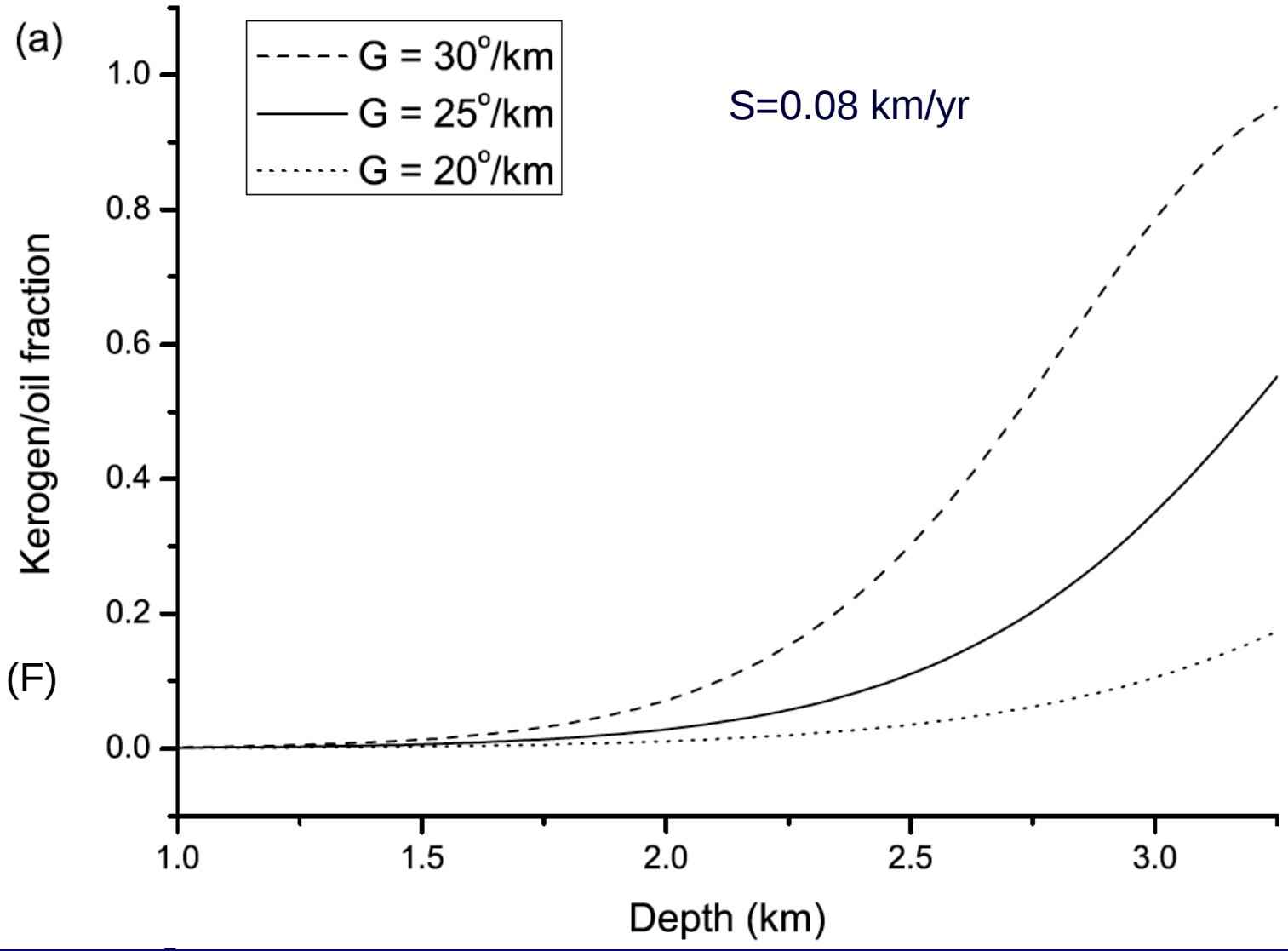

Pressure versus depth

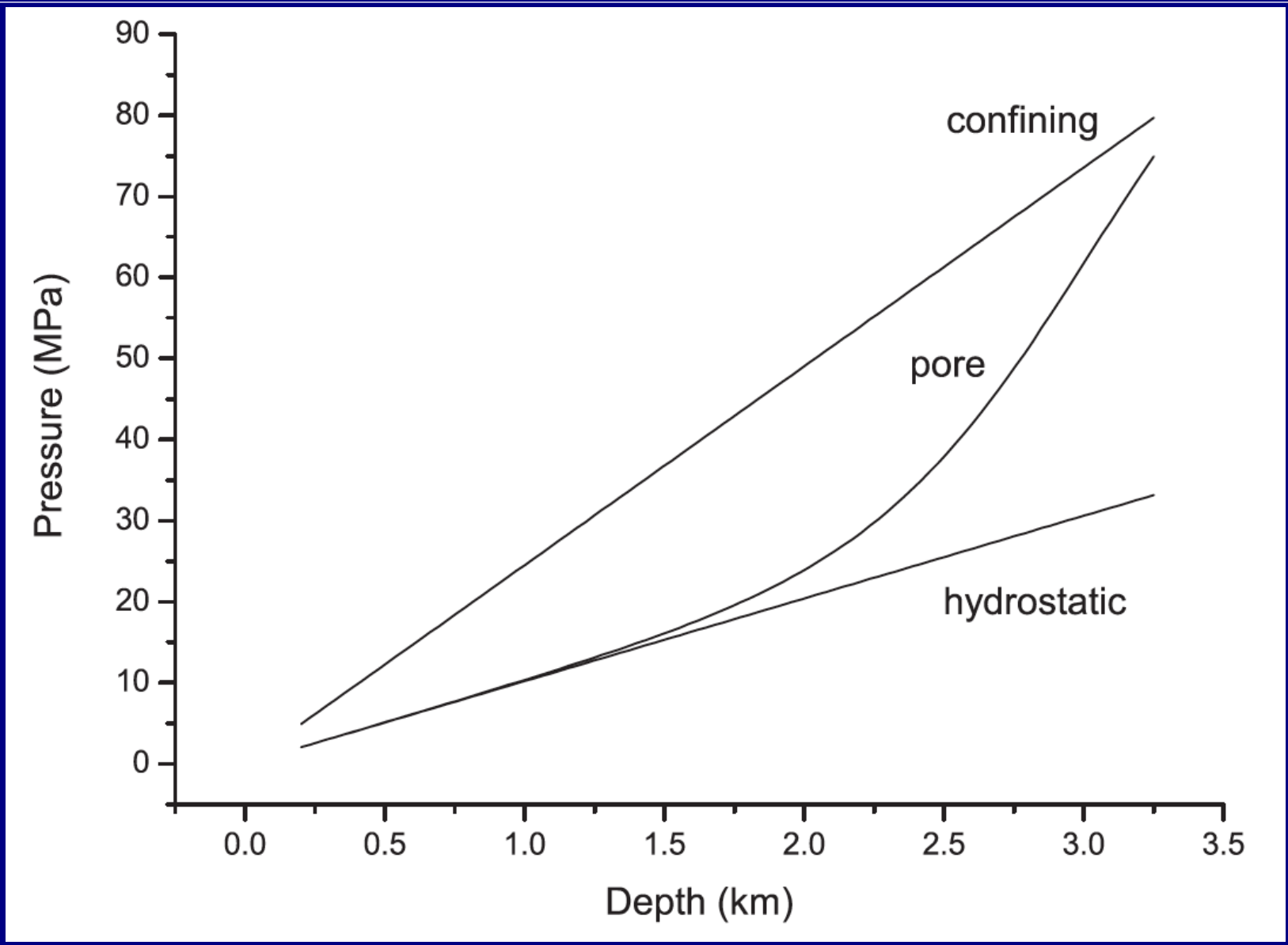

Seismic models

Anisotropy

Kerogen & Illite in sub-horizontal layering:

V_{11} - along bedding ($c_{ij} = d\ V_{ij}^2$)

V_{33} – normal to bedding

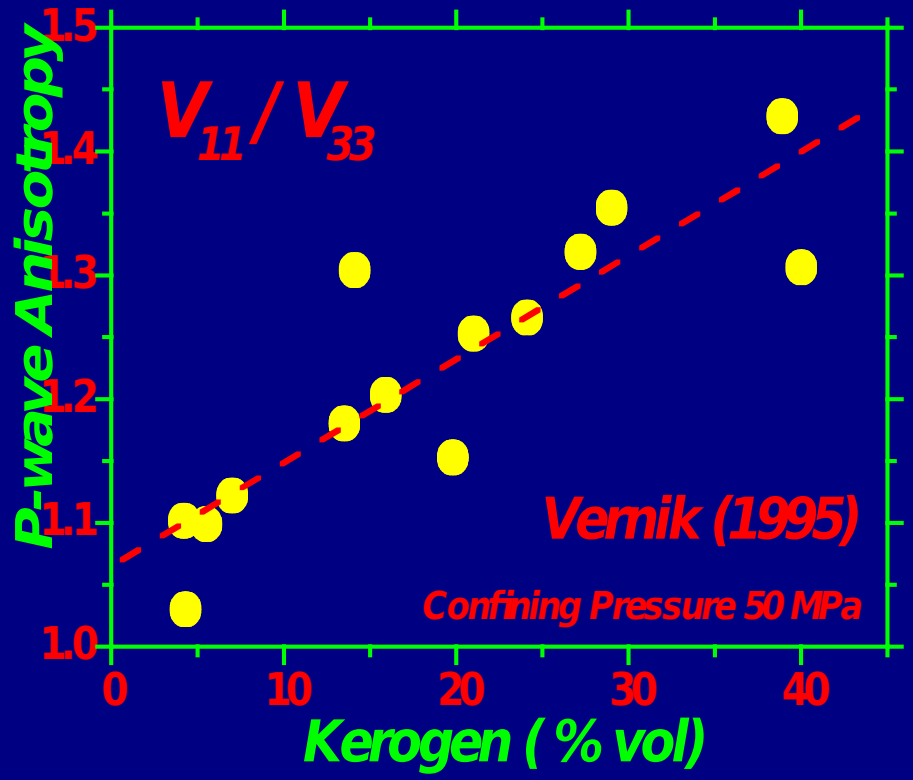

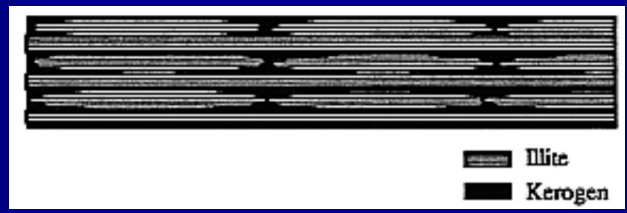

Petro-elastical model of a source rock

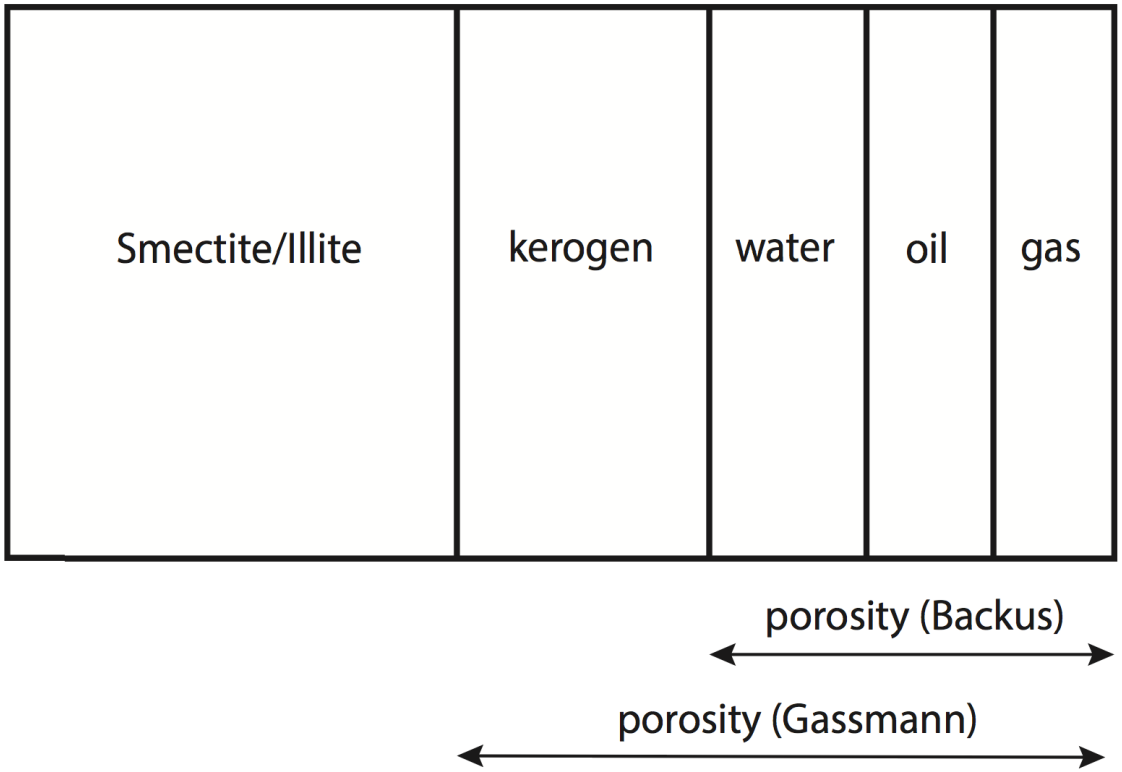

Fig. 1 Organic shale components indicating the "porosity" corresponding to the Backus and Gassmann models. The porosity in the case of the Gassmann model includes the solid pore infill. The actual porosity, ϕ, of the rock to calculate the fluid saturations is that indicated for the Backus model, i.e., the sum of the water, oil and gas proportions. The organic content porosity, ϕ_{OC}, is the sum of the kerogen, oil and gas proportions.

Petro-elastical model of a source rock

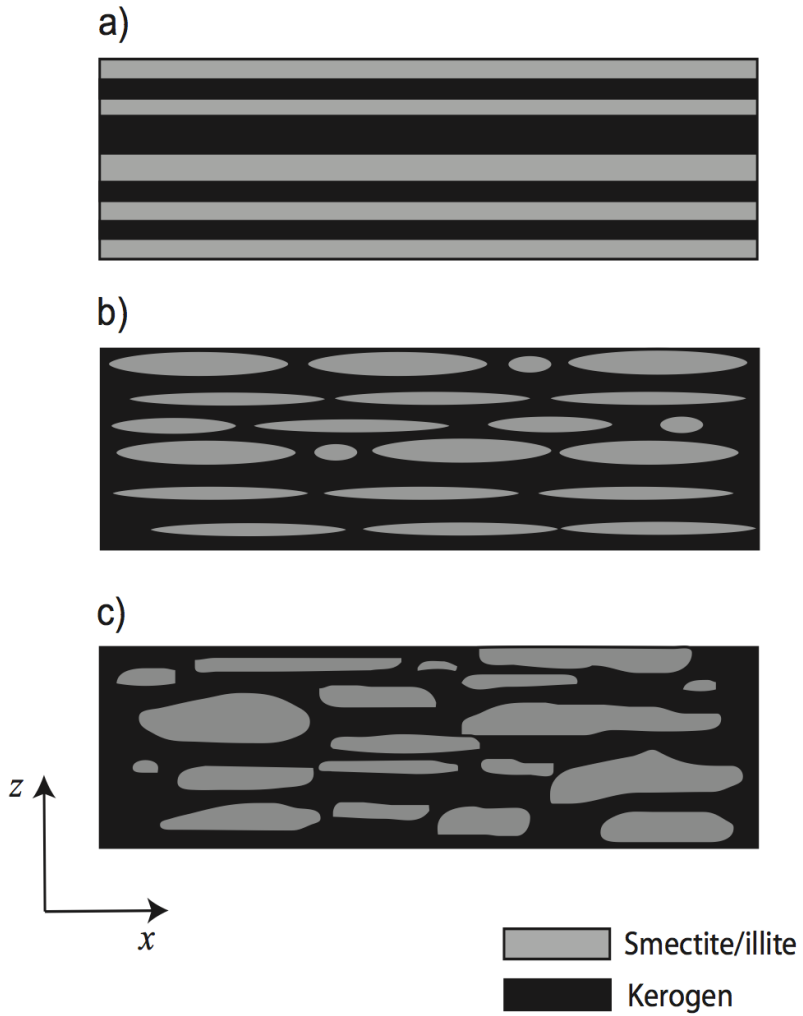

Fig. 2 Schematic fabric topology of transversely isotropic kerogen-rich shales, according to Backus model (a), modified Backus model (b) and Gassmann model (c). The z-direction corresponds to the symmetry axis.

Generalized Gassmann equation

Ciz and Shapiro (2007) obtained the undrained compliance tensor when the pore infill and solid grains are anisotropic materials,

$$\bar{s}_{ijkl} = s^m_{ijkl} - (s^m_{ijmn} - s^s_{ijmn})[\phi(\mathbf{s}^{if} - \mathbf{s}^{\phi}) + \mathbf{s}^m - \mathbf{s}^s]^{-1}_{mnqp}(s^m_{qpkl} - s^s_{qpkl}), \qquad (22)$$

Dry-rock tensor

$$s^m_{ijkl} = s^s_{ijkl} + \phi(\bar{s}_{ijmn} - s^s_{ijmn})[\phi(\mathbf{s}^{if} - \mathbf{s}^{\phi}) - \bar{\mathbf{s}} + \mathbf{s}^s]^{-1}_{mnqp}(s^{if}_{qpkl} - s^{\phi}_{qpkl}).$$

Generalization of Gassmann equations for porous media saturated with a solid material, Radim Ciz and Serge A. Shapiro, *Geophysics*, 72, no. 6, 2007, A75-A79.

Carcione, J. M., Helle, H. B., and Avseth, P., 2011, Source-rock seismic-velocity models: Gassmann versus Backus, *Geophysics*, 76, N37-N45.

Backus (Kimmeridge shale)

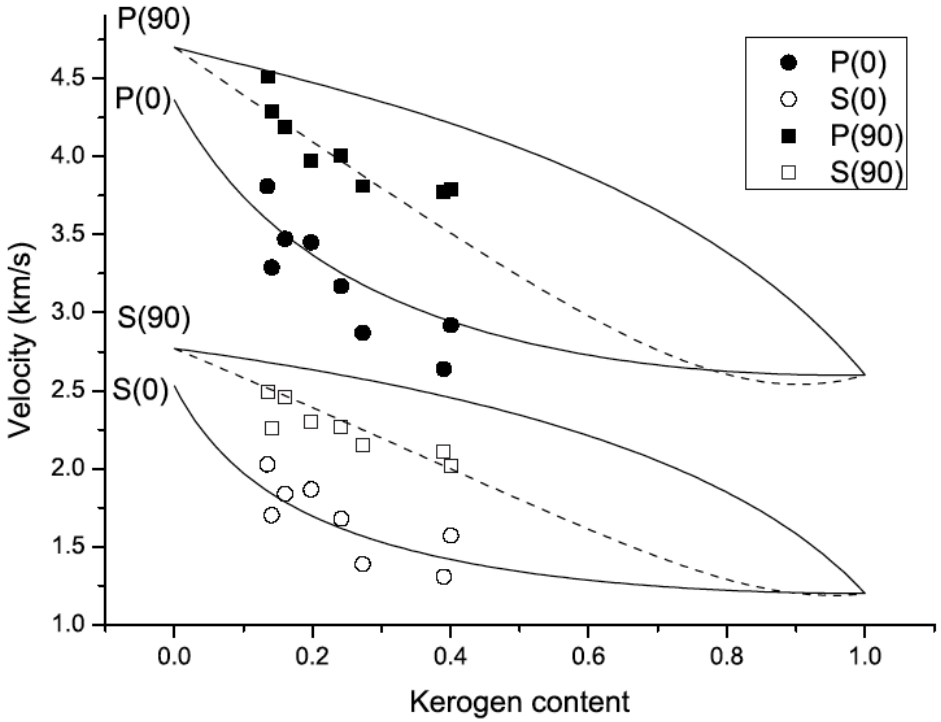

FIG. 5. Backus velocities as a function of kerogen content. The symbols correspond to the experimental data (Kimmeridge shales) (Vernik, 1995). The dashed line is the result of modifying the elastic constants of illite by assuming a lenticular textural pattern.

Gassmann (Kimmeridge shale)

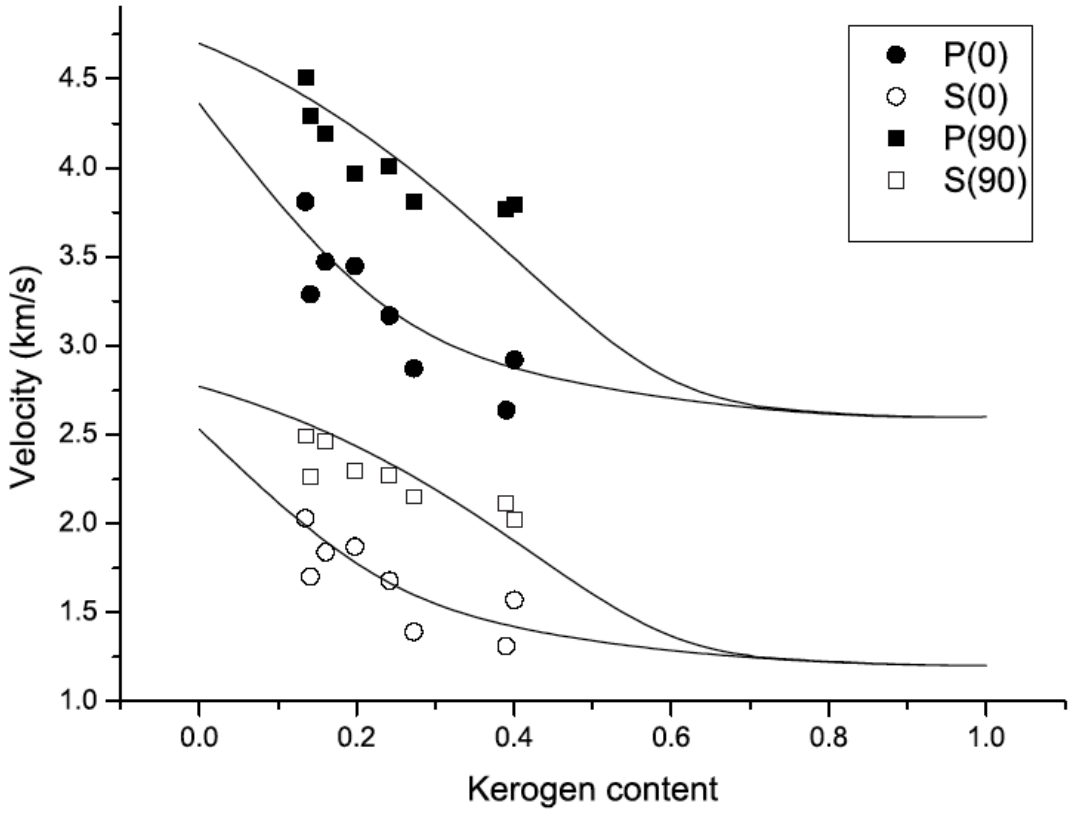

FIG. 6. Gassmann velocities as a function of kerogen, where the dry-rock moduli have been obtained by a generalization of Krief equations to the anisotropic case. The symbols correspond to the experimental data (Kimmeridge shales) (Vernik, 1995).

Calibration

Properties after calibration

Table 1. Material Properties.

Medium	Depth (km)	v_{11} (km/s)	v_{33} (km/s)	v_{55} (km/s)	v_{66} (km/s)	v_{13} (km/s)	ρ (g/cm^3)
smectite	-	2.8	2.8	1.7	1.7	1.43	2.2
illite	-	5	4.5	2.9	3.15	1.96	2.9
kerogen	2	2.7	2.7	1.5	1.5	1.7	1.2
”	3	2.7	2.7	1.5	1.5	1.7	1.4
water	2	1.66	1.66	0	0	1.66	1.04
”	3	1.65	1.65	0	0	1.65	1.02
smectite-illite-water	3	2.8	2.7	1.55	1.7	1.43	2.15
oil	3	1.11	1.11	0	0	1.11	0.73
gas	3	0.82	0.82	0	0	0.82	0.14

Diagenesis. Smectite/illite conversion

$$\frac{\partial r}{\partial t} = -r^n A \exp(-E/RT(t)),$$

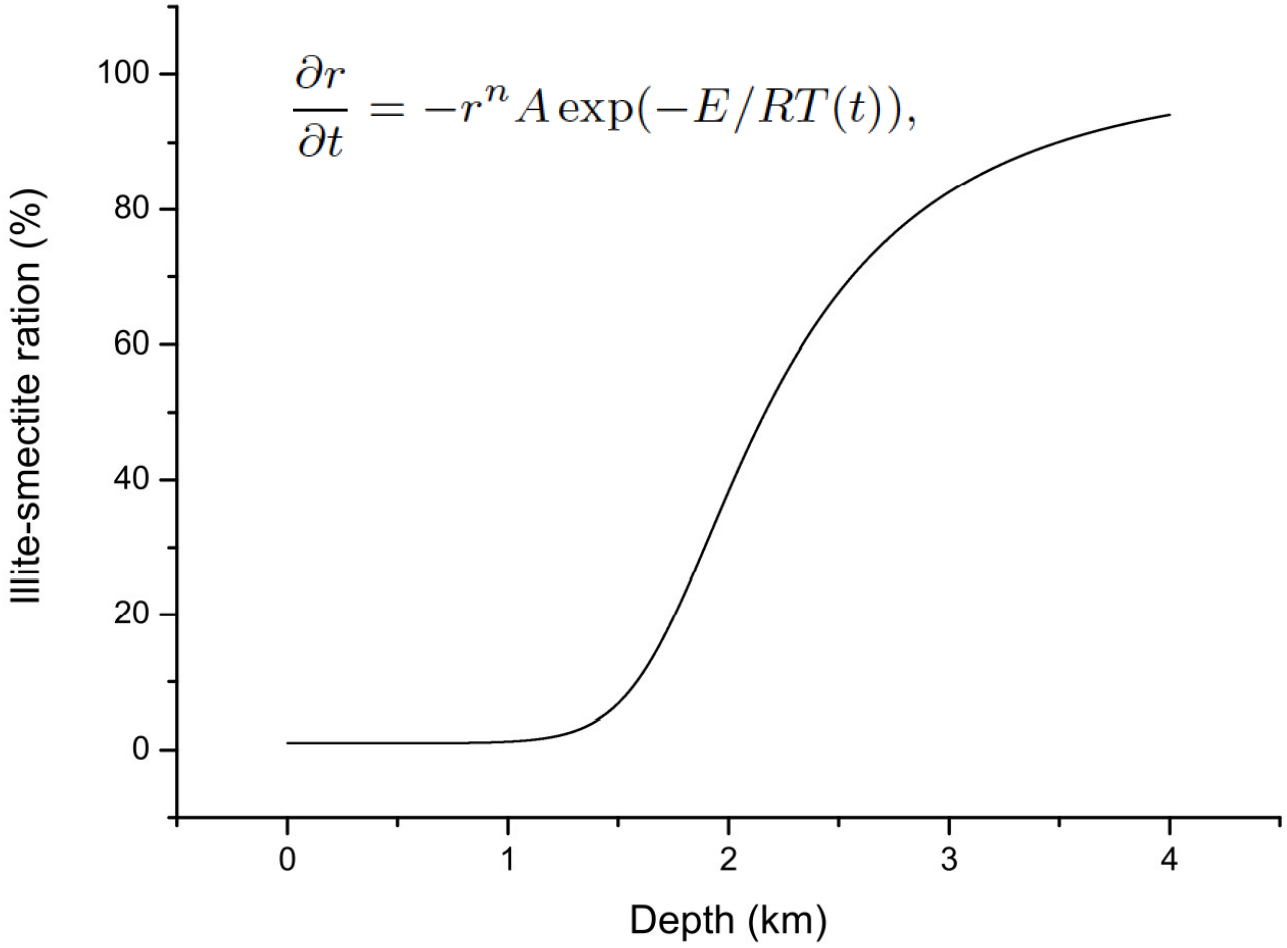

Fig. 4 Illite/smectite ratio as a function of depth.

Velocity versus depth (mineral)

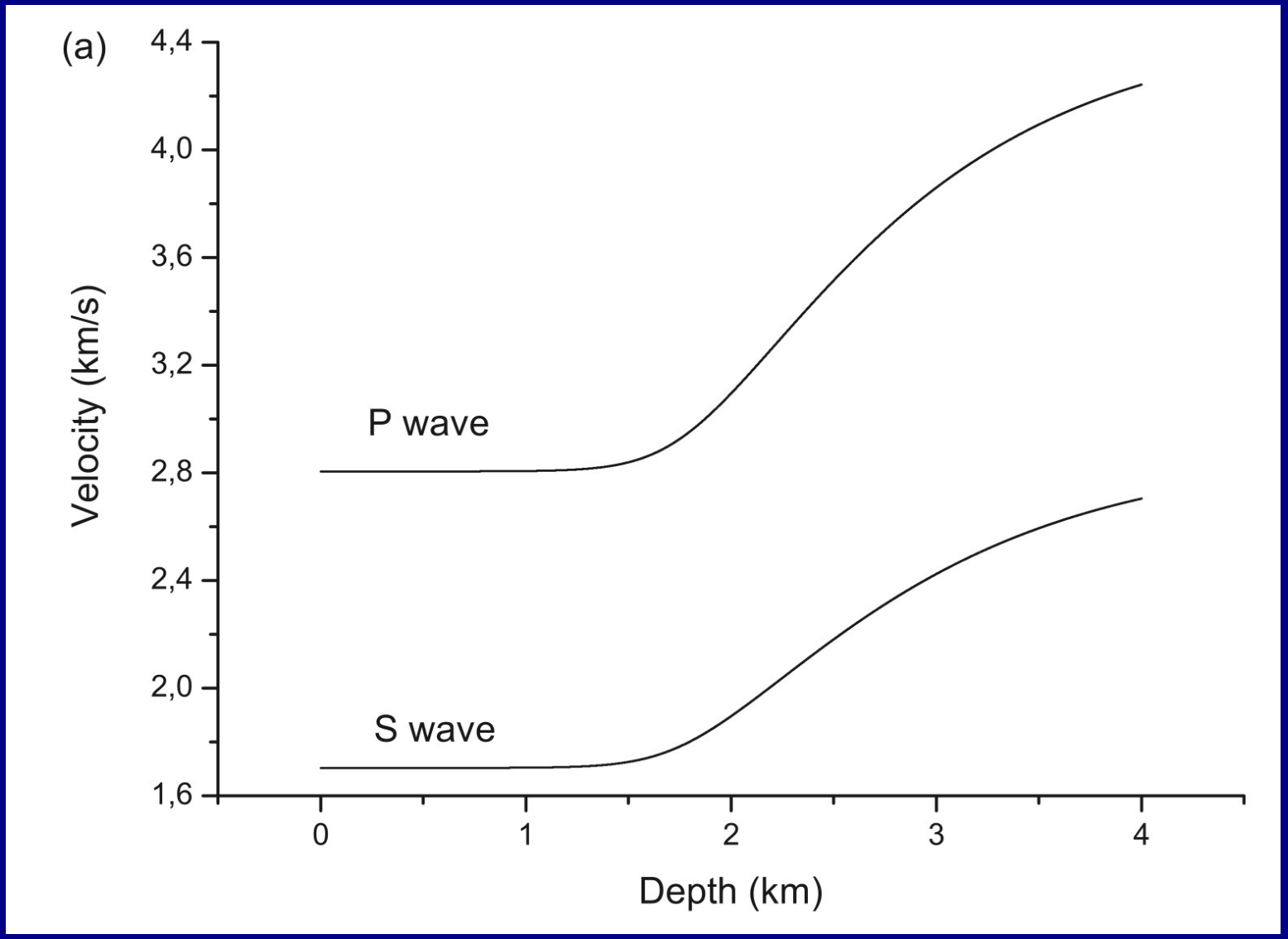

Density versus depth (mineral)

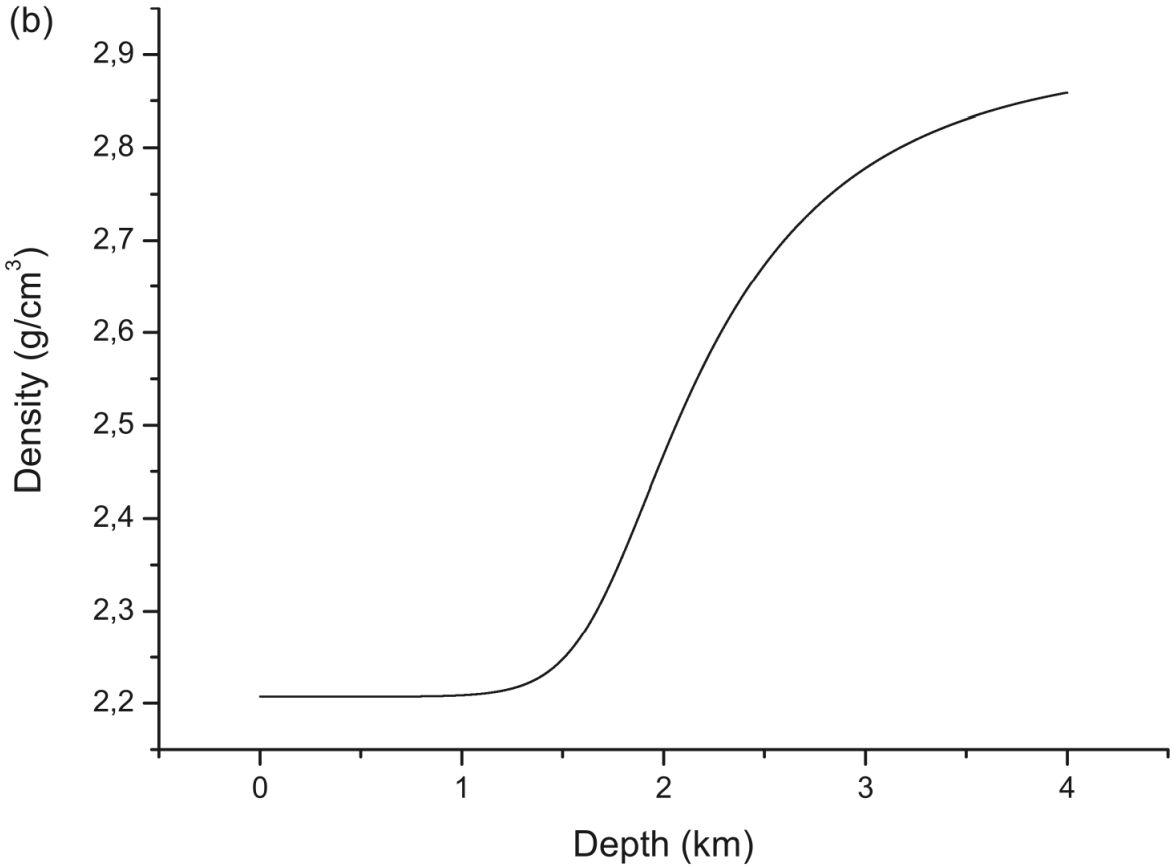

Fig. 5 Phase-velocity variations (v_{33} (P wave) and v_{55} (S wave)) (a) and mass density (b) of the mineral composing the shale frame as a function of depth due to diagenesis (smectite/illite conversion).

TOC and kerogen content

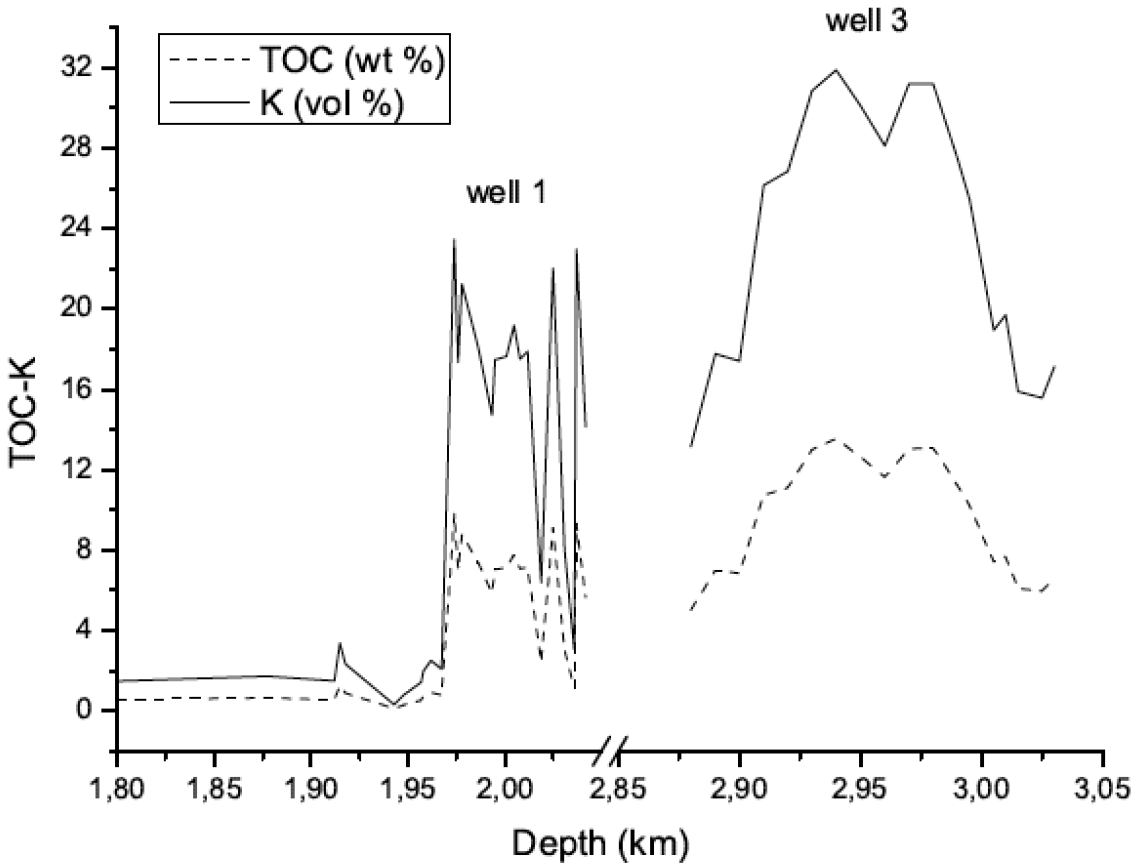

Fig. 7 TOC (in weight percent) and kerogen content K (in volume percent) corresponding to wells 1 and 3.

Porosity versus depth

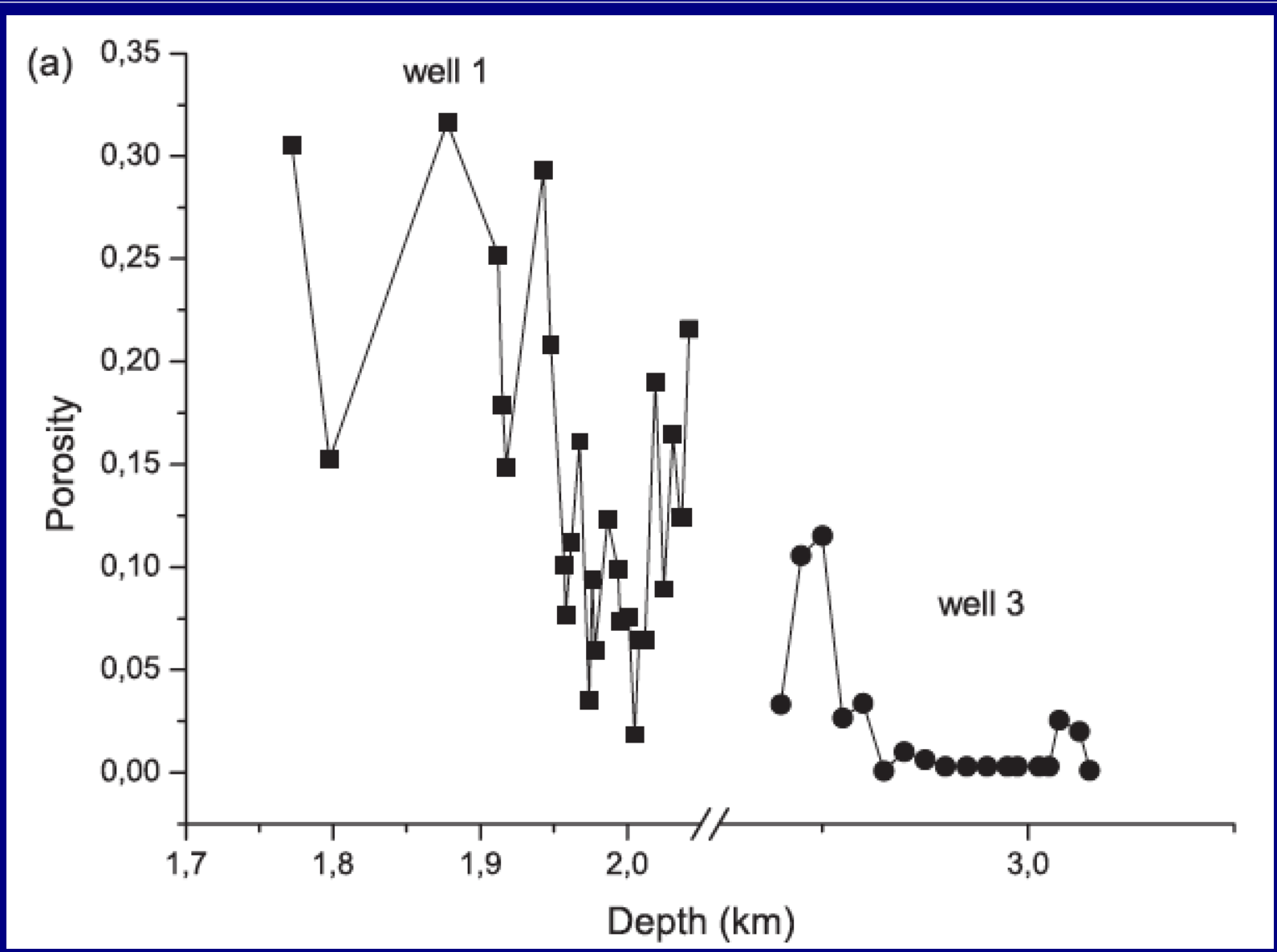

Bulk density versus depth

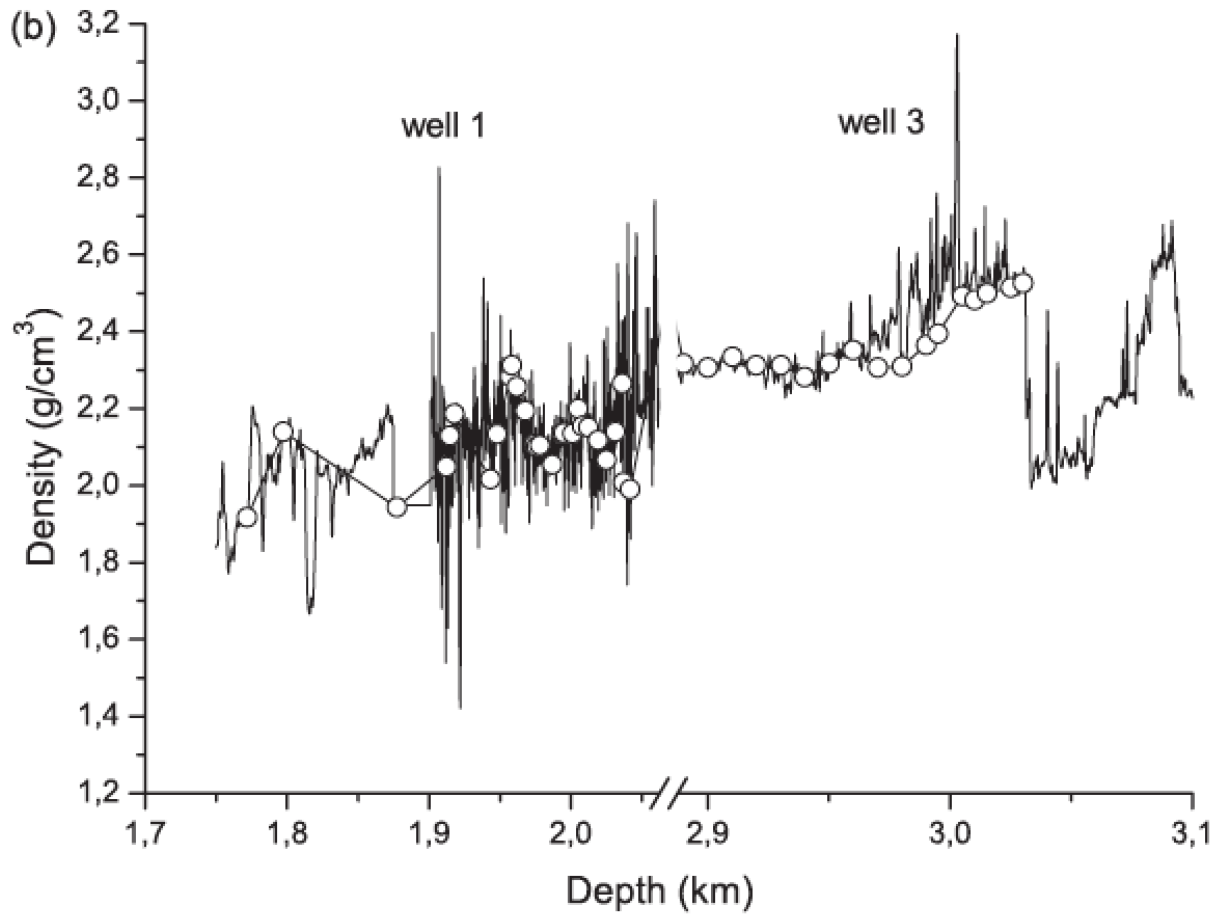

Fig. 8 Porosity (a) and bulk density (b) as a function of depth corresponding to wells 1 and 3. The open circles correspond to calculations performed with the properties given in Table 1.

Gassmann P-wave velocities

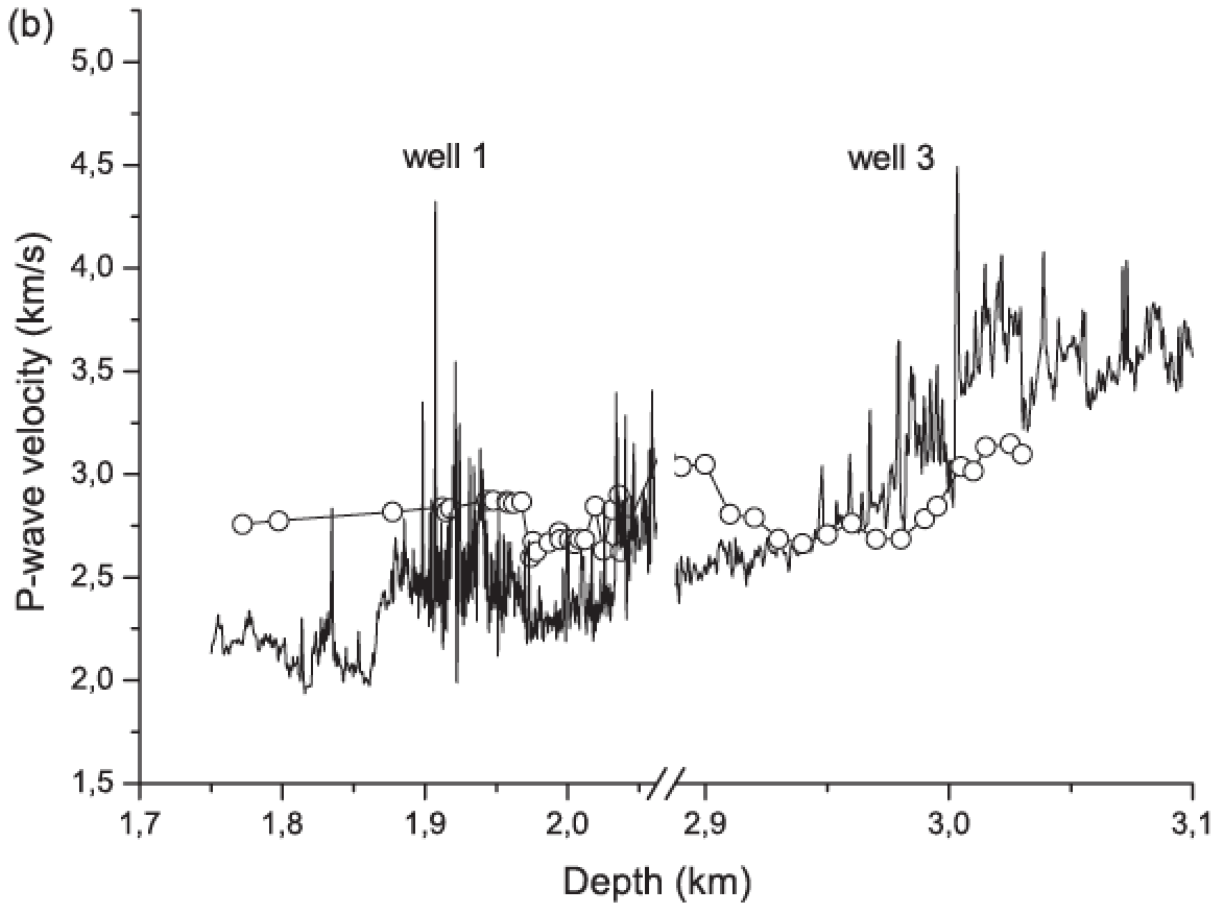

Fig. 10 Backus (a) and Gassmann (b) bedding-normal P-wave velocities as a function of depth, corresponding to wells 1 and 3. The solid lines and open circles correspond to the well-log data and model calculations at the depths indicated at the well reports, respectively.

Gassmann S-wave velocities

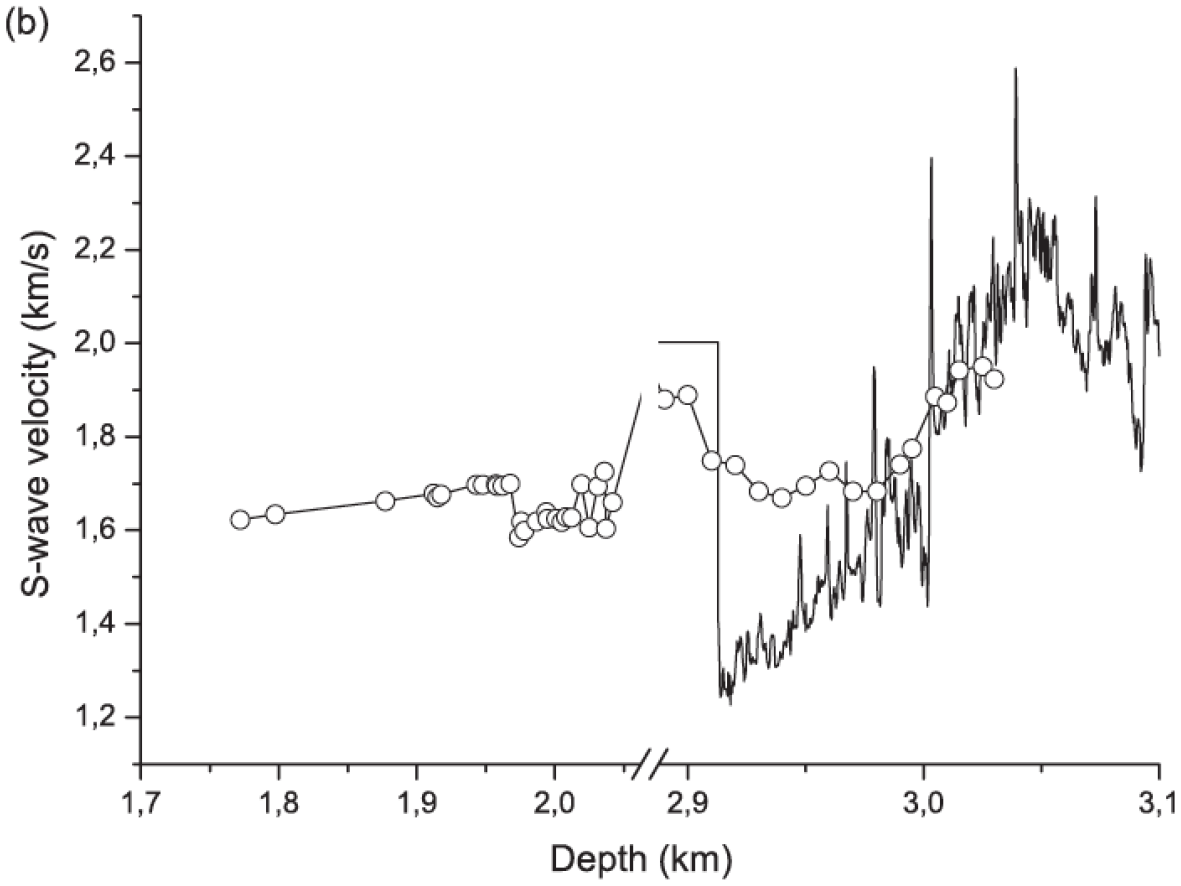

Fig. 11 Bedding-normal S-wave velocity as a function of depth, corresponding to Backus averaging (a) and Gassmann equation (b). The solid lines and open circles correspond to the well-log data and model calculations at the depths indicated at the well reports, respectively.

Thomsen anisotropy parameters

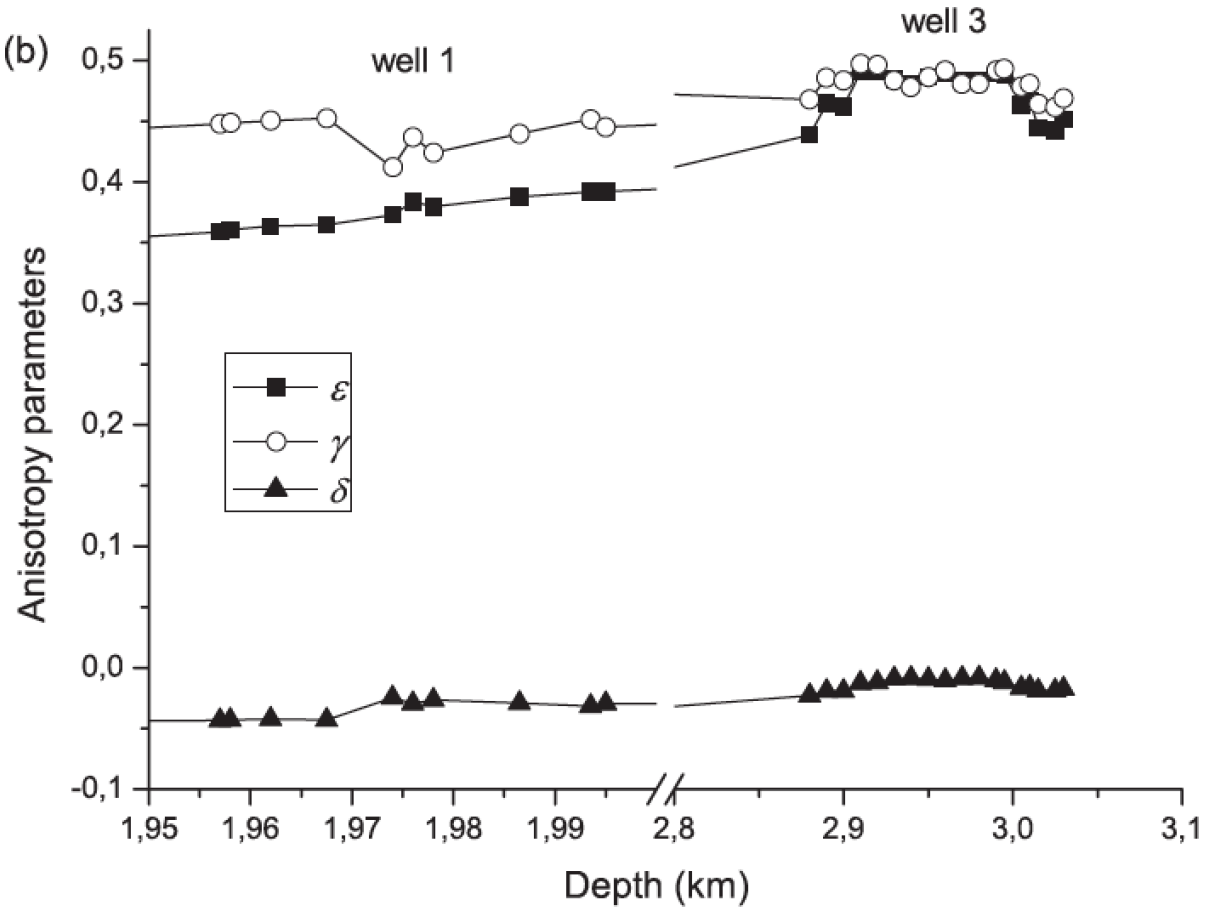

Fig. 12 Anisotropy parameters as a function of depth obtained from the Backus (a) and Gassmann (b) models, corresponding to wells 1 and 3, at the depths where TOC is given in the well reports.

Rock-physics templates

Bedding-normal P velocity (Gassmann)

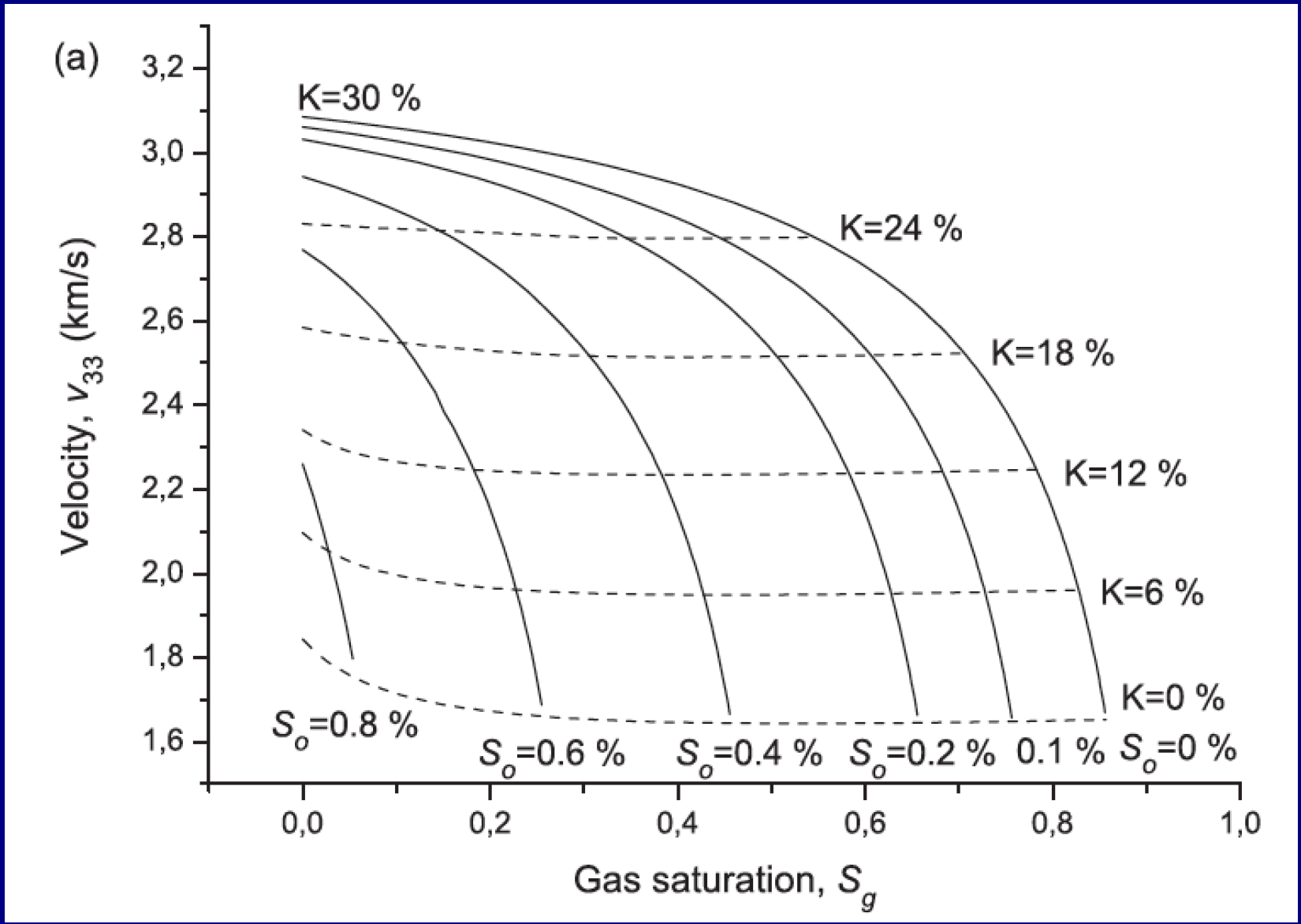

Bedding-parallel P velocity (Gassmann)

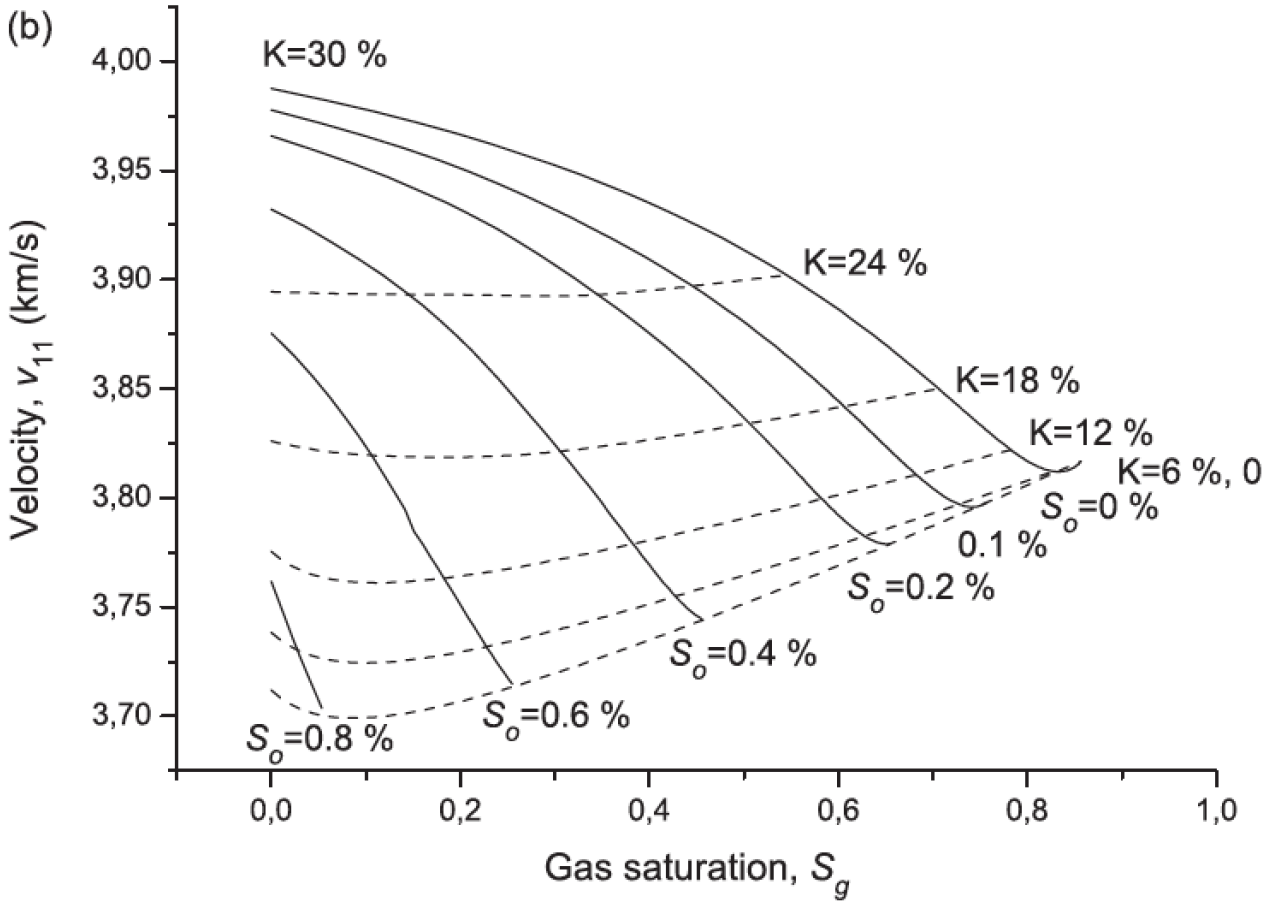

Fig. 19 Bedding-normal (a) and bedding-parallel (b) P-wave velocities as a function of gas saturation for various values of the kerogen content and oil saturations (see Figure 17). The model is Gassmann equation and the frequency is 50 Hz.

v_P/v_S versus AI (Backus)

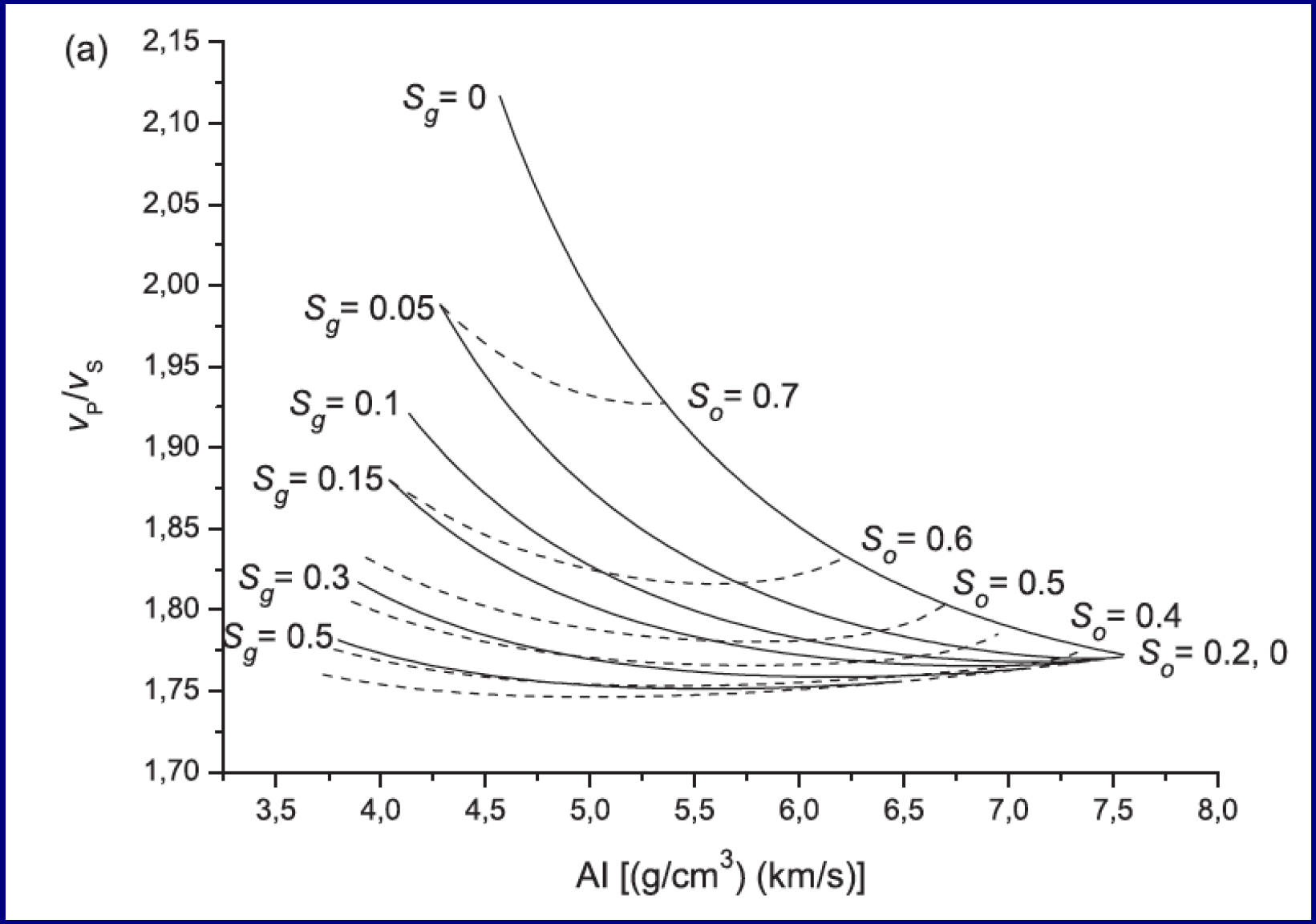

vP/vS versus AI (Gassmann)

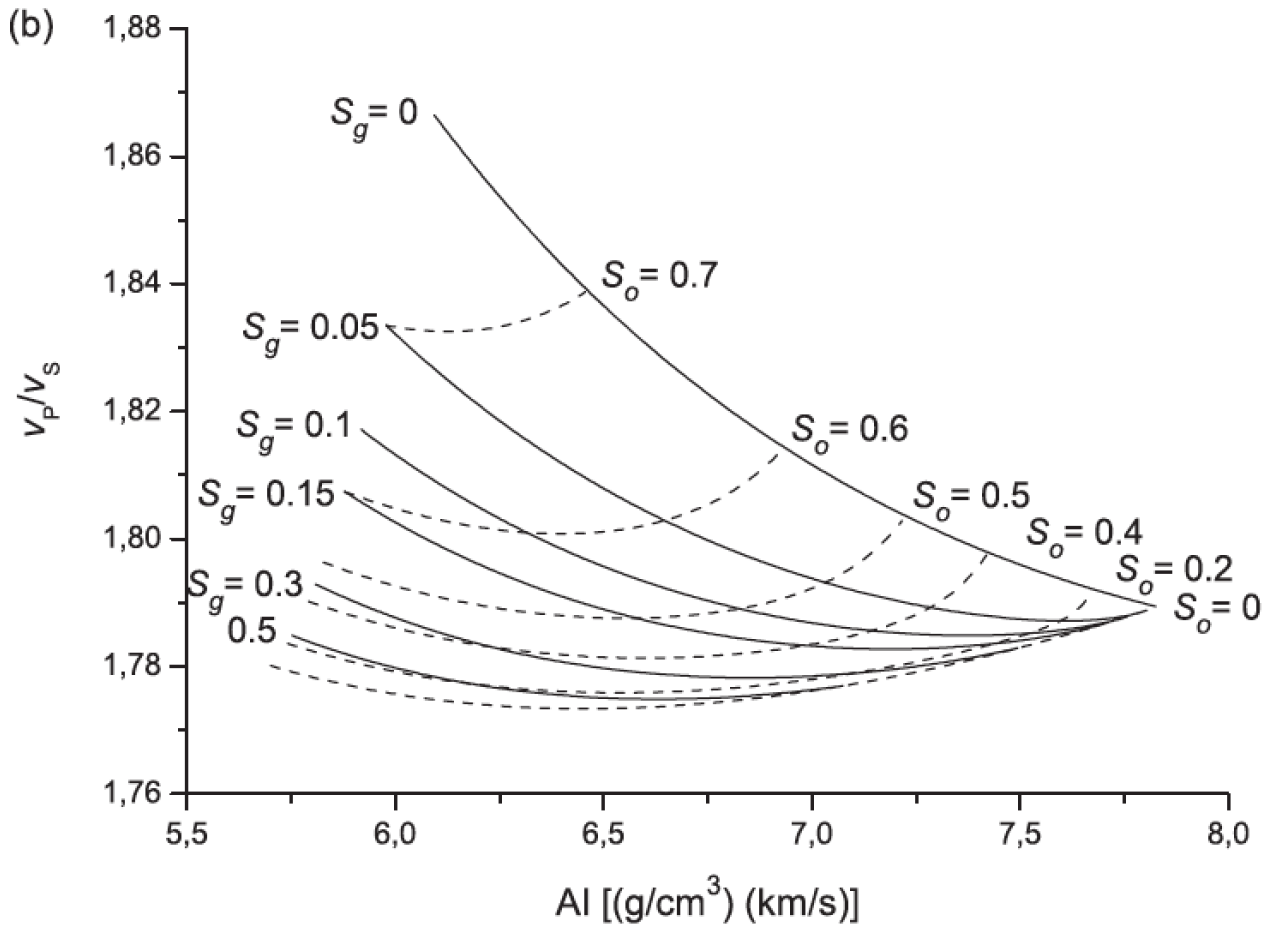

Fig. 21 v_P/v_S (v_{33}/v_{55}) as a function of the acoustic impedance (AI) for various values of the gas and oil saturations (solid and dashed lines, respectively). The models are Backus averaging (a) and Gassmann equation (b) and the frequency is 50 Hz.

Young modulus vs Poisson ratio (Backus)

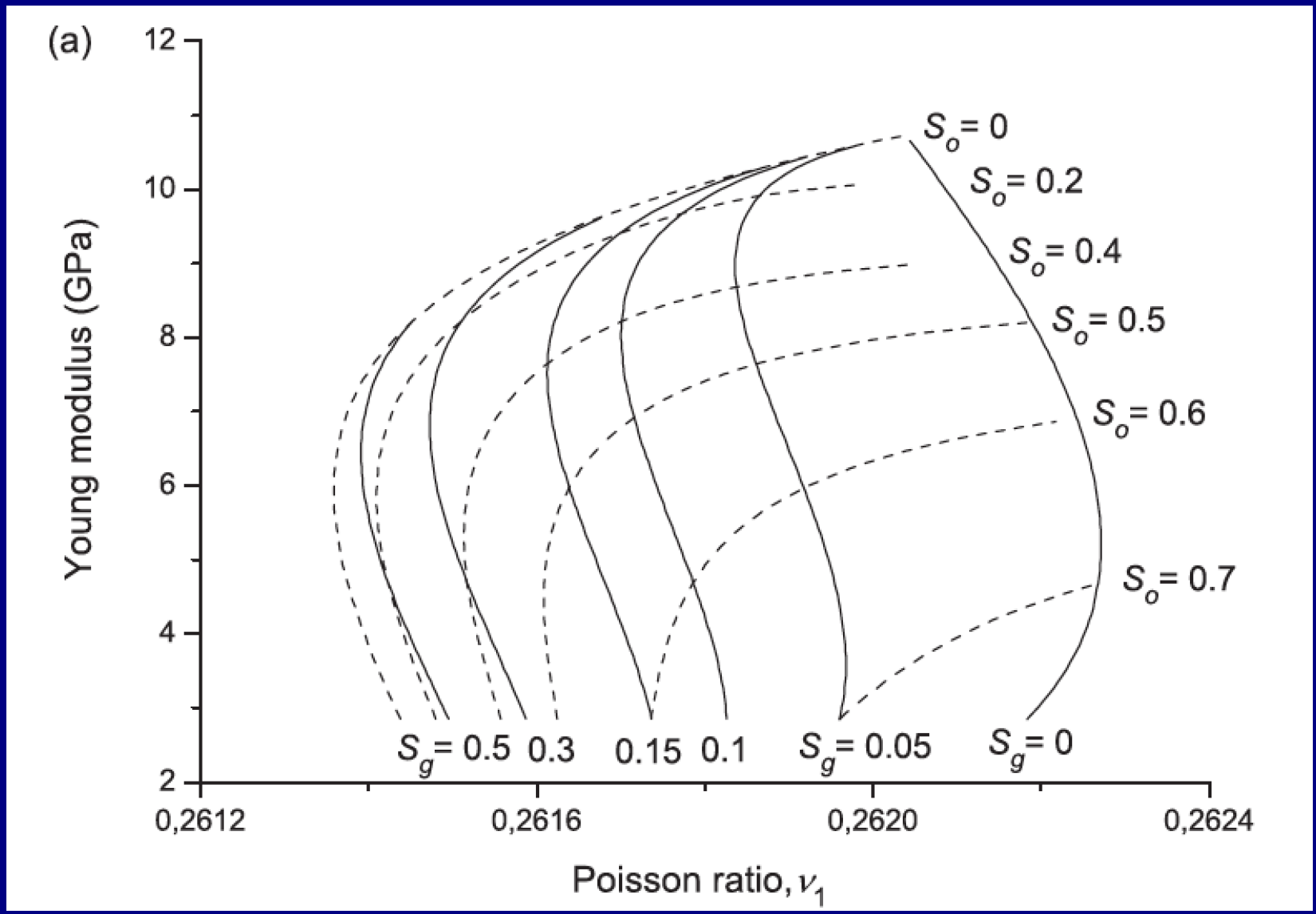

LMR (Gassmann)

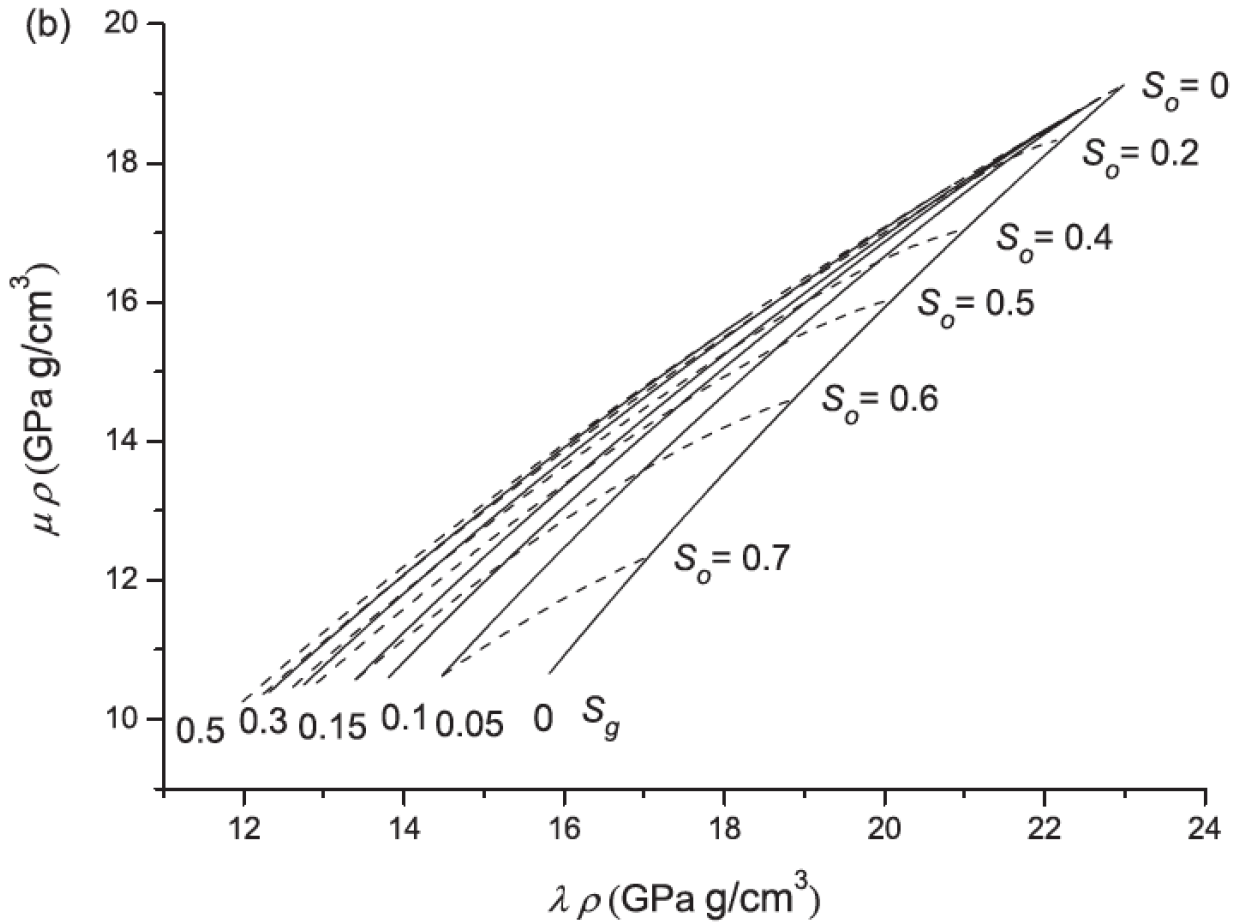

Fig. 22 λ-μ-ρ templates for various values of the gas and oil saturations (solid and dashed lines, respectively). The models are Backus averaging (a) and Gassmann equation (b) and the frequency is 50 Hz.

Rock-physics templates

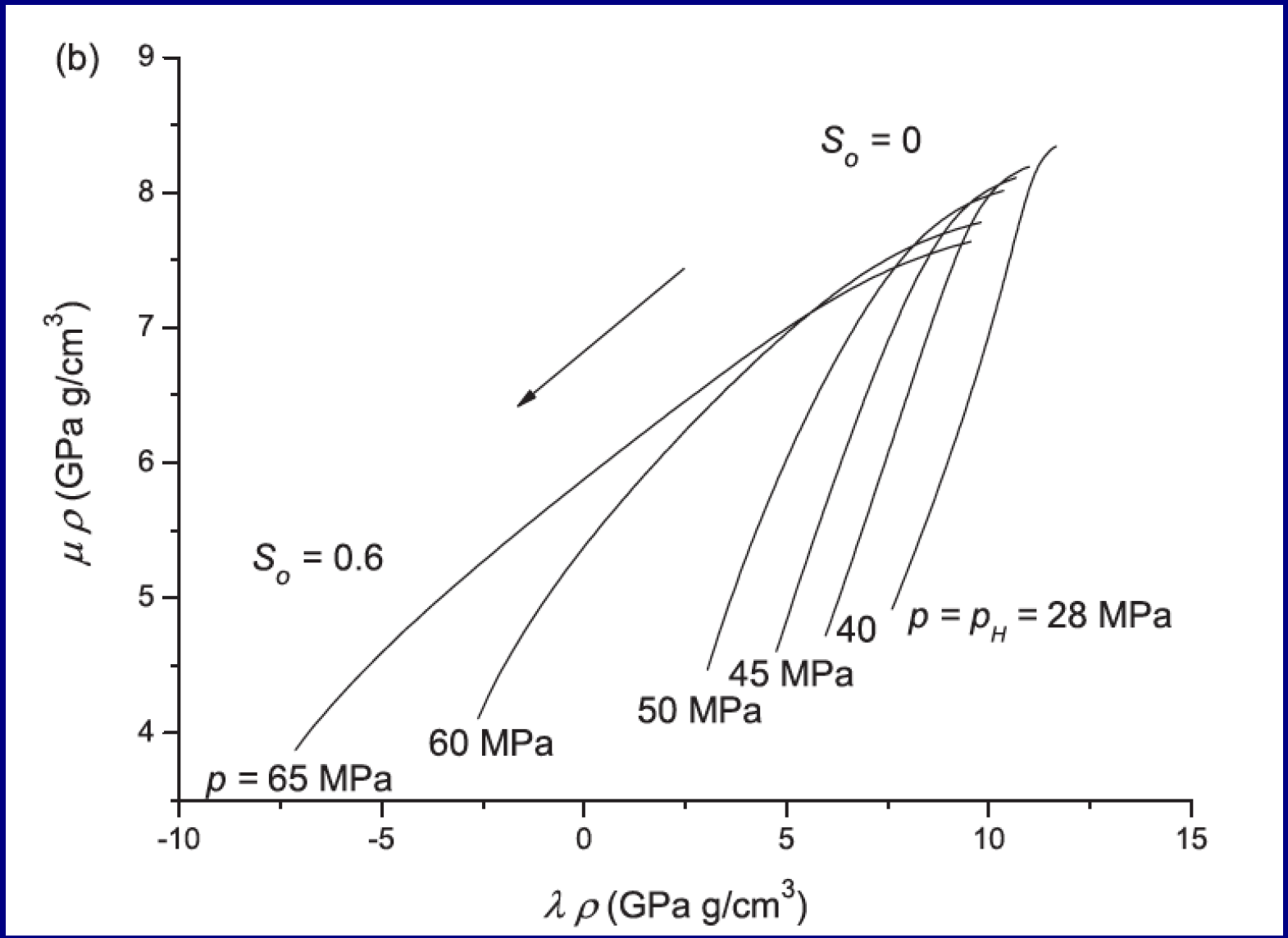

Thank you for your attention

Truth is ever to be found in the simplicity, and not in the multiplicity and confusion of things.

Isaac Netwon

1817

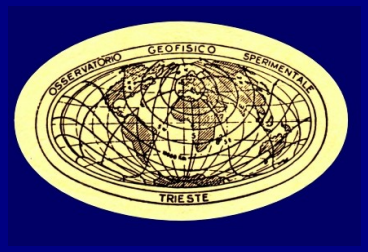

1921

1989

2012

LMR (Gassmann) – Pressure template

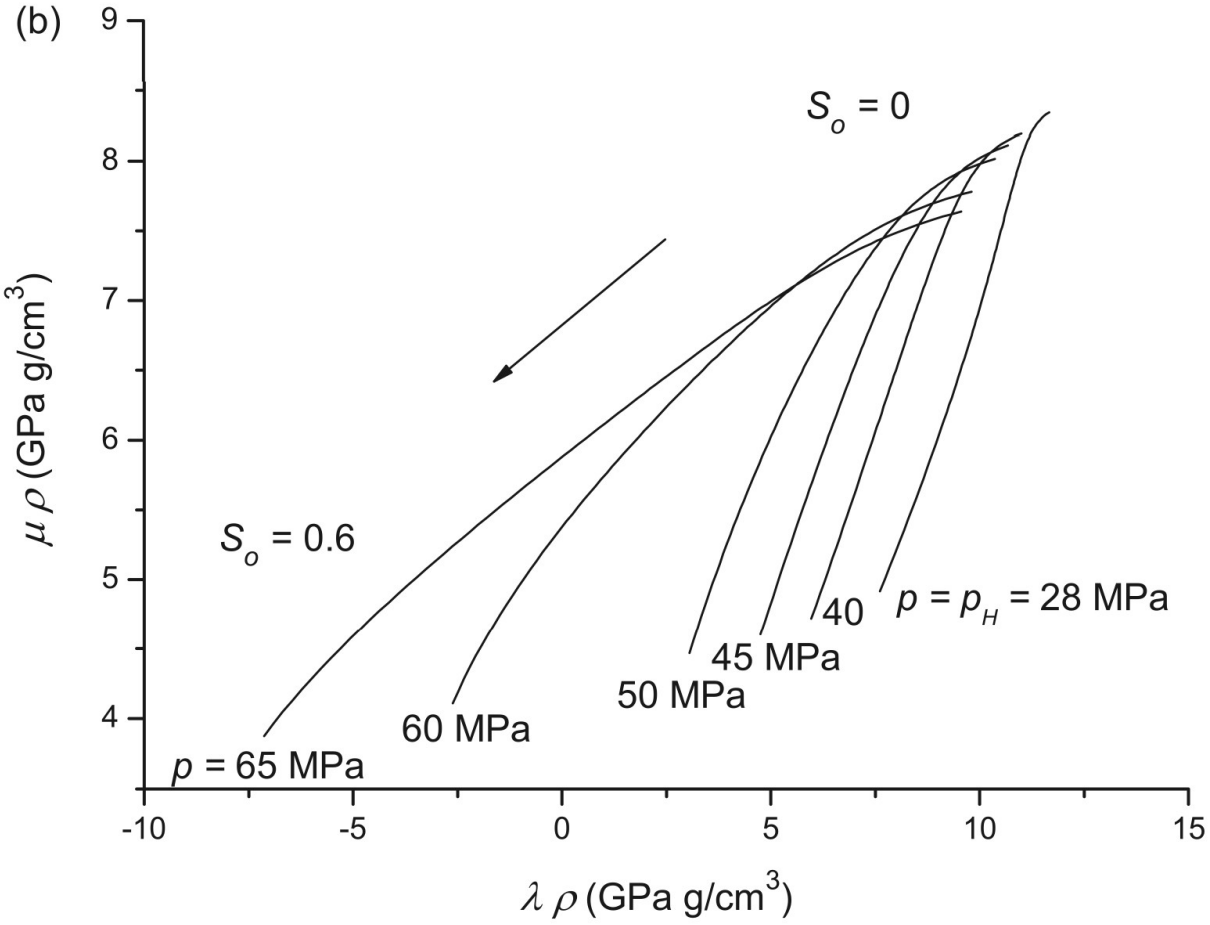

Fig. 23 v_P/v_S (v_{33}/v_{55}) as a function of the acoustic impedance (AI) (a) and λ-μ-ρ template for different values of the pore pressure and varying oil saturation. The model is Gassmann equation and the frequency is 50 Hz.

v_P/v_S versus AI (Gassmann) Pressure template

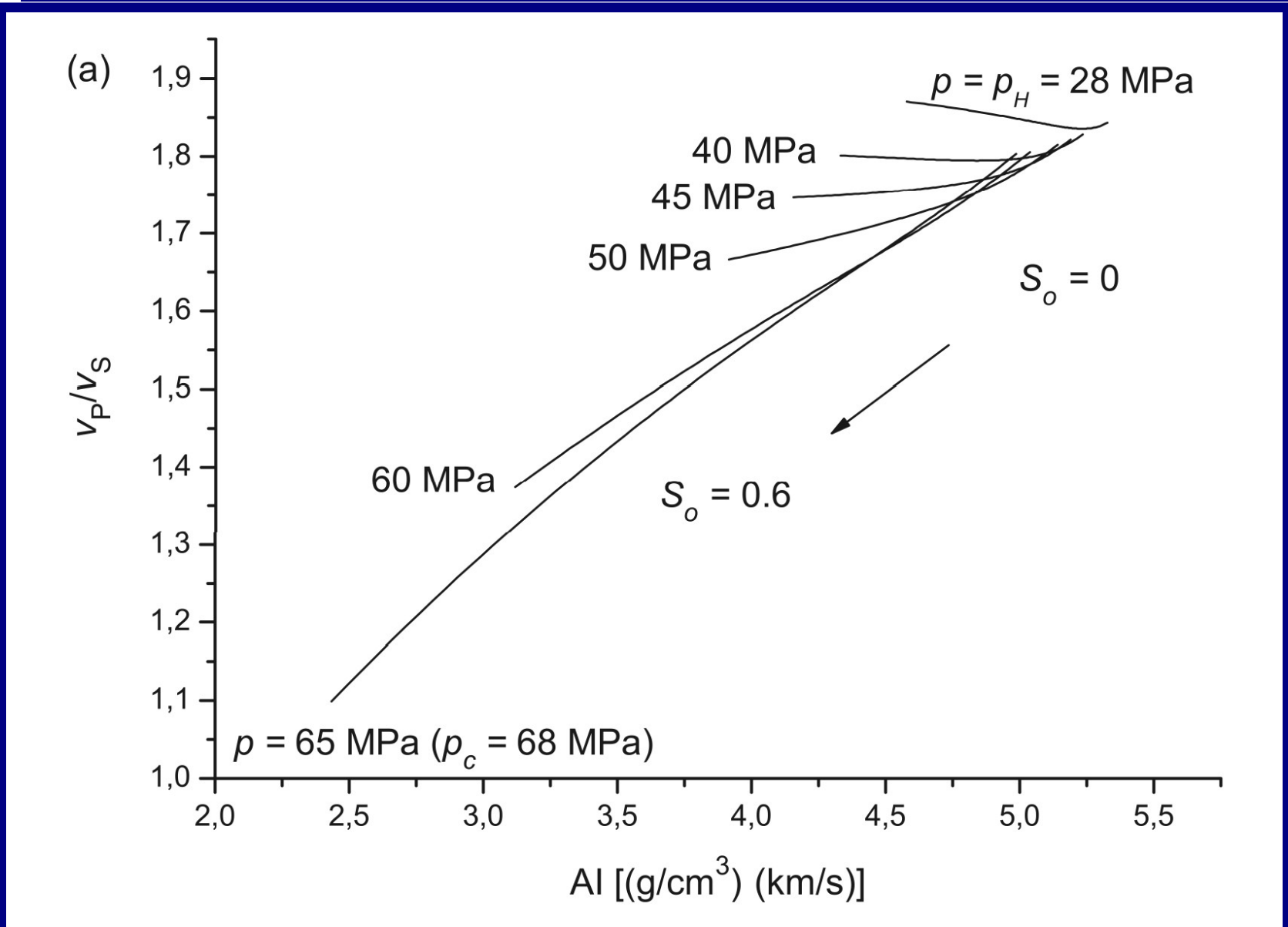

TOC (predicted from densities)

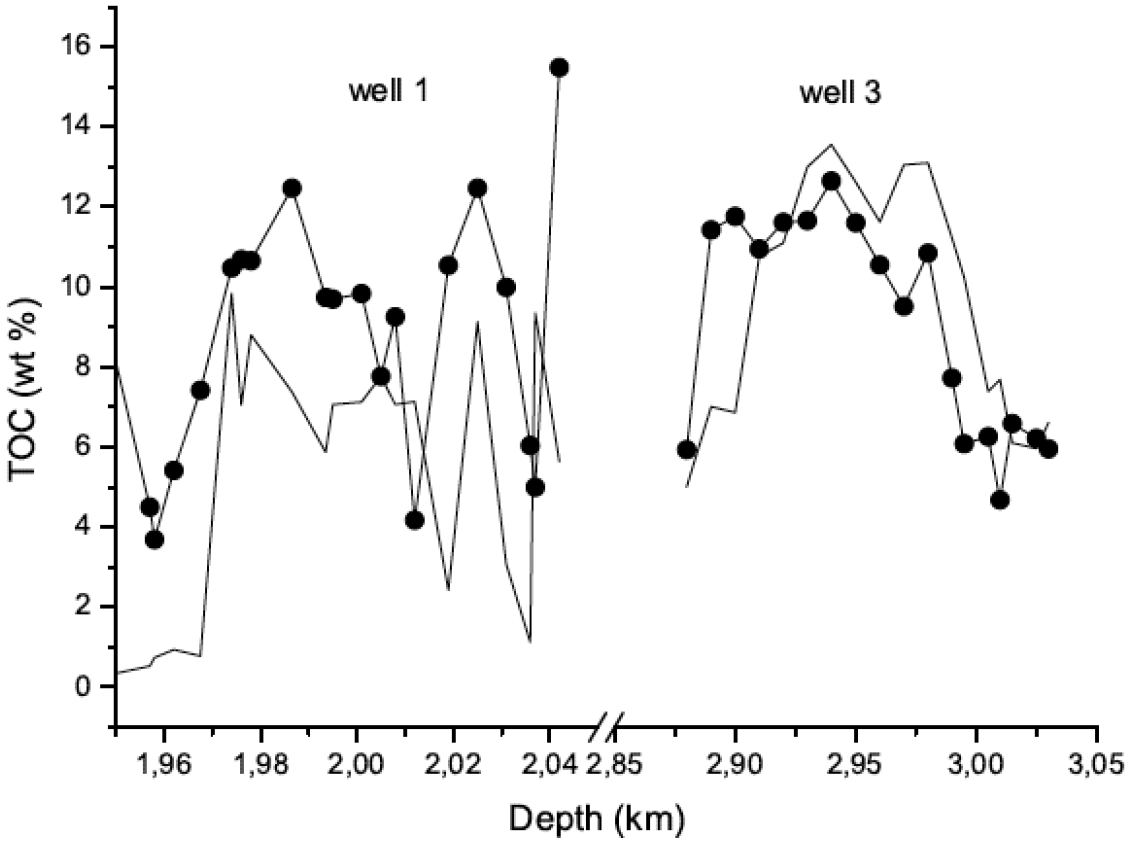

Fig. 9 TOC (in weight percent) from well reports (solid line) and predicted by equation 9 (full circles), corresponding to wells 1 and 3.